Zootaxa 5786 (1): 406–422
https://www.mapress.com/zt/

Article

ISSN 1175-5326 (print edition)
ZOOTAXA
ISSN 1175-5334 (online edition)

https://doi.org/10.11646/zootaxa.5786.1.34
http://zoobank.org/urn:lsid:zoobank.org:pub:322023CE-DD7E-47D8-A5FB-3545199D5CC0

Four new species of the genus *Blaps* Fabricius, 1775 from Xizang, China (Coleoptera: Tenebrionidae: Blaptinae: Blaptini)

BAO-YUE ZHANG[1,2], XIN-YU LI[1,3] & XIU-MIN LI[1,4*]
[1]*Key Laboratory of Zoological Systematics and Application of Hebei Province; College of Life Sciences, Hebei University, Baoding, Hebei, 071002, China*
[2] *BaoyueZhang0112@163.com; https://orcid.org/0009-0008-9251-479*
[3] *lixinyu01313@163.com; https://orcid.org/0009-0009-0400-0132*
[4] *lixiumin@hbu.edu.cn; https://orcid.org/0000-0003-0575-1869*
[*]*Corresponding author*

Abstract

With 214 species, the genus *Blaps* Fabricius, 1775 is one of the most diverse genera of the tribe Blaptini. In this study, we reconstructed a preliminary phylogenetic tree based on cytochrome *c* oxidase subunit I (*COI*) sequences from 41 species, and 38 species belong to the subgenera *Ablapsis* Reitter, 1887, *Blaps* Fabricius, 1775 and *Nalepa* Reitter, 1887 from China. Furthermore, four new species from Xizang, China are described and illustrated: *Blaps* (*Blaps*) *miranda* Li, **sp. nov.**, *B*. (*Ablapsis*) *tuberculata* Li, **sp. nov.**, *B*. (*A*.) *asperula* Li, **sp. nov.** and *B*. (*A*.) *gracilis* Li, **sp. nov.** In addition, a key to 18 species of the subgenus *Ablapsis* is provided. The results of the phylogenetic analyses suggest that the nominotypical subgenus is likely paraphyletic, indicating a need for further phylogenetic studies to clarify the status of the various subgenera.

Key words: darkling beetles, molecular phylogenetics, new taxa, taxonomy

Introduction

The subtribe Blaptina Latreille, 1817 consists of 10 genera, comprising about 350 species (Chigray & Kirejtshuk 2023). The genus *Blaps* Fabricius, 1775 is the most species-rich genus within the subtribe Blaptina, encompassing 214 species worldwide, with a primary distribution in the Palaearctic region (Nabozhenko & Chigray 2020; Chigray & Kirejtshuk 2023; Zhang & Li 2025). Reitter (1887) initially proposed *Ablapsis* Reitter, 1887 and *Nalepa* Reitter, 1887 as subgenera within the genus *Blaps.* Later he elevated both subgenera to generic rank (Reitter 1893). Medvedev (2001) argued the inclusion of *Ablapsis* as a subgenus of *Blaps*, suggesting the addition of several species from the subgenus *Prosoblapsia*. Chigray and Kirejtshuk (2023) concurred with Medvedev's assessment, mentioned similarities in aedeagal structure between *A. compressipes* Reitter, 1887, and certain species of the subgenus *Prosoblapsia* Skopin & Kaszab, 1978, thereby supporting the classification of these species as a subgenus within the genus *Blaps*. Furthermore, Chigray and Kirejtshuk (2023) proposed *Lithoblaps* Motschulsky, 1860 as a distinct genus, transferring 100 species and subspecies from *Blaps* to *Lithoblaps* based on morphological differences in imaginal and larval structures.

Zhang & Li (2025) proposed the reinstatement of *Nalepa* as a subgenus of *Blaps* Fabricius, 1775 based on the results of phylogenetic analyses. Currently, the genus *Blaps* comprises five subgenera: *Ablapsis* Reitter, 1887 (21 spp./ssp.), *Arenoblaps* G. S. Medvedev, 1999 (one sp.), *Blaps* Fabricius, 1775 (182 spp./ssp.), *Dineria* Motschulsky, 1860 (two spp.), and *Nalepa* Reitter, 1887 (eight spp.). The nominotypical subgenus exhibits the highest species diversity within the genus, followed by *Ablapsis*. Notably, 95 species from three subgenera are found in China, with significant levels of endemic species richness observed around the Qinghai-Xizang Plateau (Ren *et al.* 2016; Chigray & Kirejtshuk 2023; Zhang & Li 2025).

 Accepted by Z.-W. Yin: 11 Jul. 2025; published: 1 Apr. 2026

In this study, we verified the taxonomic status of four new species based on morphological characteristics and the results of a molecular phylogenetic analysis including new molecular data generated for this study. The steady influx of new molecular data is laying the foundations for future research into the origin and evolution of species diversity in Blaptini.

Material and methods

Morphological examination

In total, 29 specimens belonging to four new species were examined for this study and deposited at the Museum of Hebei University, Baoding, China (MHBU). The photographs were taken with the following imaging system: Canon EOS 5D Mark III (Canon Inc., Tokyo, Japan) connected to a Laowa FF 100 mm F2.8 CA-Dreamer Macro 2× or Laowa FF 25 mm F2.8 Ultra Macro 2.5–5× (Anhui Changgeng Optics Technology Co., Hefei, China). Multiple images were stacked to construct the final figures. Montaged images were edited using Adobe Photoshop v. 22.1.0 to form the final figure plates. Label data are presented verbatim. A slash (/) separates text on different lines of label.

Taxon sampling, DNA extraction, PCR amplification, and sequencing

Specimens were collected during fieldwork in Xizang, China. Detailed information for all the samples used in this study (including those without molecular data) is provided in Table S1.

DNA was extracted from leg muscle tissue of adults using the Insect DNA Isolation Kit (BIOMI-GA, Hangzhou, China) following the manufacturer's protocols. The DNA extracted was stored at -20°C. Fragments of the cytochrome *c* oxidase subunit I (*COI*) mitochondrial gene were amplified with the primers F2183 and R3014 (Folmer *et al*. 1994). The profile of the PCR amplification consisted of an initial denaturation step at 94°C for 4 min, 35 cycles of denaturation at 94°C for 1 min, annealing for 45 s, an extension at 72°C for 1 min, and a final 8 min extension step at 72 °C. PCR was performed using TaKaRa Ex Taq (TaKaRa, Dalian, China). PCR products were subsequently checked by 1% agarose gel electrophoresis and sequencing was performed at General Biol Co. (Anhui, China). Detailed information for the samples used this study is provided in Table S1.

Phylogenetic analyses

In total, 103 sequences from 38 *Blaps* species were used for the phylogenetic analyses. This dataset consists of 79 published sequences and 24 new sequences from nine species, including four new species. We also used previously published sequences of four species from the genus *Oodescelis* Motschulsky, 1845 within the tribe Platyscelidini Lacordaire, 1859) as the outgroups, which was considered to be sister to the tribe Blaptini (Medvedev 2001, Egorov 2009, Kamiński *et al.* 2021).

Phylogenetic analysis was based on the *COI* gene fragment under maximum likelihood (ML). The best-fit model was determined according to the corrected Akaike's Information Criterion (AICc) using ModelFinder (included in IQ-TREE) with PhyloSuite v. 1.2.2 (Zhang *et al*. 2020). The ML tree search was performed in IQ-TREE v. 1.6.8 (Nguyen *et al.* 2015). The best-score ML tree was obtained using a heuristic search implementing 1000 random-addition replicates with a random-starting tree, and the 'Substitution Model Auto+R6' option for all partitions of dataset. Clade support was assessed using ultrafast bootstrap replicates (Minh *et al.* 2013; 1000 replicates); ultrafast bootstrap values (uBV) above or equal to 95% were considered as strongly supported following authors' recommendations. The consensus phylogenetic tree was visualized in Figtree v. 1.4.4 (http://tree.bio.ed.ac.uk/software/figtree, accessed 2025-4-1).

Results

Phylogenetic relationships

The final IQ-TREE analysis yielded a topology based on *COI* sequences (667 bp), and the preliminary phylogenetic relationships were hypothesized from 103 samples, representing 34 known and four new species of genus *Blaps* (Fig. 1). In-group individuals were classified into seven clades: Clade C1, Clade C2, Clade C3, Clade C4, Clade C5, Clade C6 and Clade C7. Six species of the subgenus *Nalepa*, corresponded to the well-supported Clade C1 (uBV = 100%). Eight known species and three new species (*B.* (*A.*) *tuberculata* Li, **sp. nov.**, *B.* (*A.*) *asperula* Li, **sp. nov.** and *B.* (*A.*) *gracilis* Li, **sp. nov.**) of the subgenus *Ablapsis* corresponded to the well-supported Clade C2 (uBV = 91%). All species of Clade C3 (uBV = 75%), Clade C4 (uBV = 70%) and Clade C5 (uBV = 69%) comprised six known species and one new species (*B.* (*B.*) *miranda* **Li, sp. nov.**) of the subgenus *Blaps* distributed in the Tibetan Plateau, corresponded to the low-supported. All species of Clades C6 (uBV = 100%) and Clade C7 (uBV = 99%) of subgenus *Blaps* were distributed in northwest China and corresponded to the well-supported.

Key to the species of the subgenus *Ablapsis* from China based on males

1. With elytral mucro 2
- Without elytral mucro. 3
2. Elytral with thick transverse ridges . . . . . ***B. transversimsulcata transversimsulcata***
- Elytral without transverse ridge . . . . . ***B. latericosta***
3. Pronotum with granules, prosternal process with one sharp nubble at apex . . . . . ***B. breiti***
- Pronotum with punctations, prosternal process without sharp nubble at apex. 4
4. Antennomere VII thick and short, length almost as long as width; pronotum transverse . . . . . ***B. brevis***
- Antennomere VII slender, length longer than width; pronotum as wide as long 5
5. Sides of pronotum with one or two flat depressions . . . . . ***B. helleri***
- Sides of pronotum without flat depression. 6
6. Antennomeres VIII–X long spherical. 7
- Antennomeres VIII–X spherical. 12
7. Apex of elytral obtusely rounded (greater than 90 degrees) . . . . . ***B. gracilis* sp. nov.**
- Apex of elytral acute (less than 90 degrees). 8
8. Disc of elytra with granules 9
- Disc of elytra with punctations or wrinkles 10
9. Parameres strongly curved in lateral view, obviously “C”-shaped . . . . . ***B. berezowskii***
- Parameres nearly straight in lateral view . . . . . ***B. tuberculata* sp. nov.**
10. Lateral margin of parameres nearly parallel in dorsal view. . . . . ***B. compressipes***
- Lateral margin of parameres not parallel in dorsal view 11
11. Parameres widest at base, triangular or conical-shaped; lateral margin of parameres weakly narrowing from base to apex in dorsal view . . . . . ***B. socia socia***
- Parameres widest at base and 1/3 of apex, gourd-shaped; lateral margin of parameres concave in dorsal view. . . . . ***B. allardiana allardiana***
12. Disc of elytra with wrinkles 13
- Disc of elytra with granules or punctations 14
13. Pro- and mesotibiae straight . . . . . ***B. brevipes***
- Pro- and mesotibiae concave . . . . . ***B. asperula* sp. nov.**
14. Elytra with punctations. 15
- Elytra with granules or particle 16
15. Elytral disc flat, with three flat ridges on each elytron. . . . . ***B. apicecostata***
- Elytral disc convex, without ridges on each elytron. . . . . ***B. himalaica***
16. Parameres conical-shaped, weakly converging from base to apex . . . . . ***B. gentilis gentilis***
- Parameres needle-shaped, lateral margins slightly emarginated from base to middle, then weakly converging from middle to apex. 17
17. Pronotum nearly smooth, with blurred punctures; elytra finely granulated, distinctly at apex . . . . . ***B. conica***
- Pronotum with coarse sculpture and dense punctures; elytra with dense granulated. . . . . ***B. holcus***

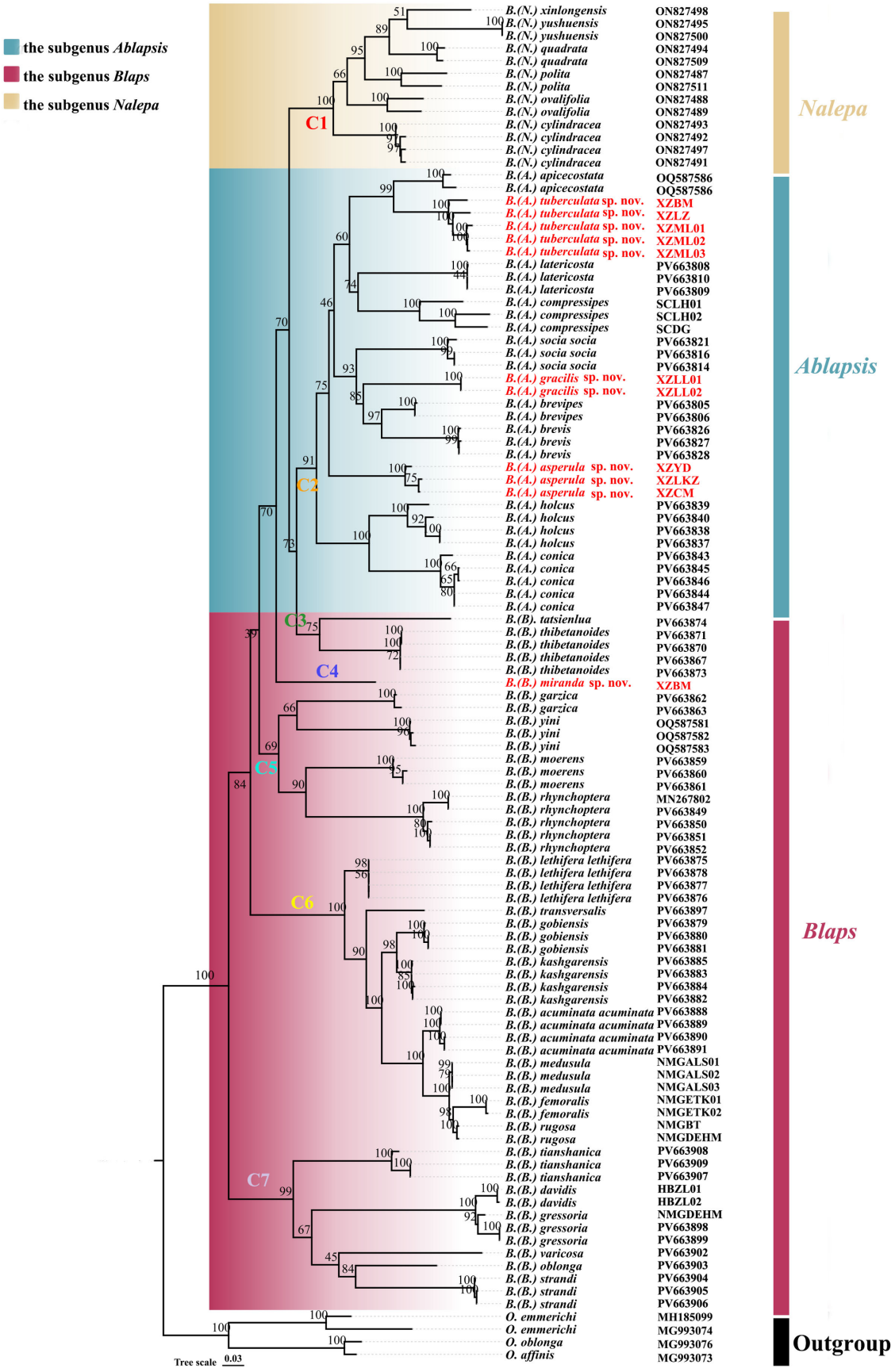

FIGURE 1. Maximum-likelihood phylogenetic tree based on 667 bp *COI* sequences within *Blaps*.

***Blaps* (*Blaps*) *miranda* Li, sp. nov.**
urn:lsid:zoobank.org:act:A805F29C-5572-4893-A040-9E9661D64AB8

Type material. HOLOTYPE: CHINA: ♂ **(MHBU):** 'Yi'ong Township, Bomê County, Xizang/ 30.2578°N, 94.8925°E/ Alt 2427m/ 31.VII.2021/ Guo-dong Ren leg.'. **PARATYPES: CHINA:** 1 ♂, 2 ♀♀ (in ethanol) (MHBU), same data as holotype; 1 ♀ (in ethanol) (MHBU): 'Mêdog County, Xizang/ Alt 2111m/ 11.VIII.2016/ Zhi-Lin Chen leg.'; 1 ♀ (in ethanol) (MHBU): 'Baxoi County, Xizang/ 30.0383°N, 95.2594°E/ Alt 2413m/ 23.VIII.2018/ Guo-dong Ren leg.'; 1 ♀ (in ethanol) (MHBU): 'Bomê County, Xizang/ 30.2691°N, 94.8162°E/ Alt 2230m/ 30.VII.2021/ Guo-dong Ren leg.'; 1 ♀ (in ethanol) (MHBU): 'Bomê County, Xizang/ Alt 2304m/ 22. VIII.2017/ Xiao-Dong Yang leg.'.

Description. *Male* (Figs 2, 3A–C). Body oval-oblong, length 16.5–17.5 mm, width 6–7 mm; dull black, rough, convex.

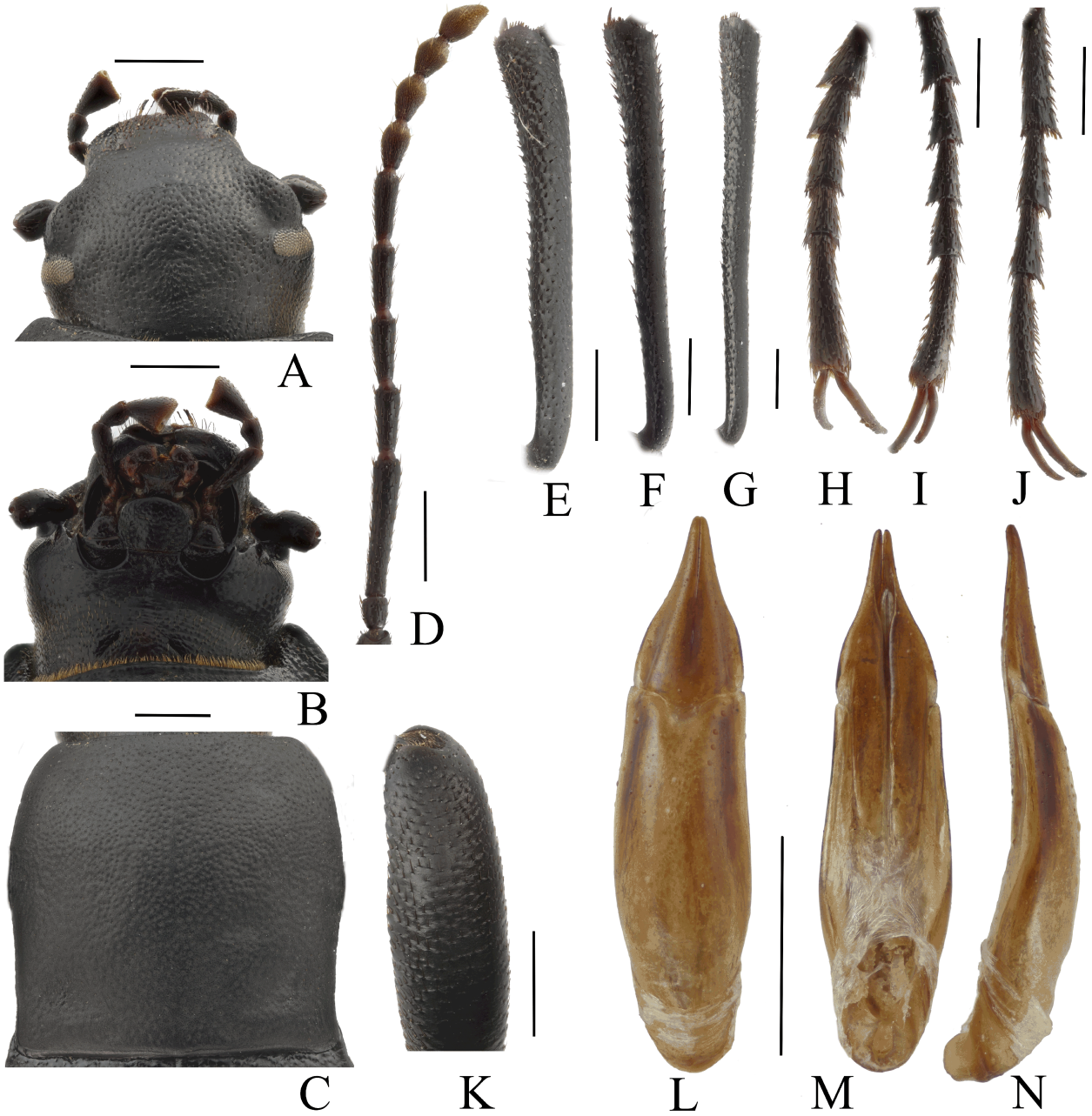

FIGURE 2. *Blaps (Blaps) miranda* Li, **sp. nov. A.** Head, dorsal view. **B.** Head, ventral view. **C.** Pronotum. **D.** Antenna. **E.** Protibia. **F.** Mesotibia. **G.** Metatibia. **H.** Protarsus. **I.** Mesotarsus. **J.** Metatarsus. **K.** Profemur, apical part. **L–N**. Aedeagus: dorsal (L), ventral (M), lateral (N). Scale bars: 1.0 mm.

Head (Fig. 2A, B). Anterior margin of epistome straight. Head convex, with coarse puncturation. Mentum transversely oval. Antennae long, antennomere VII reaching base of pronotum when directed backward, antennomeres III–VII cylindrical, VIII–X long spherical, XI spindle (Fig. 2D). Ratio of length (width) of antennomeres II–XI 5.3 (4.5): 23.4 (4.2): 10.3 (4.2): 10.0 (4.1): 10.8 (4.1): 11.2 (4.2): 7.5 (4.6): 7.1 (5.1): 6.6 (5.2): 8.3 (5.3).

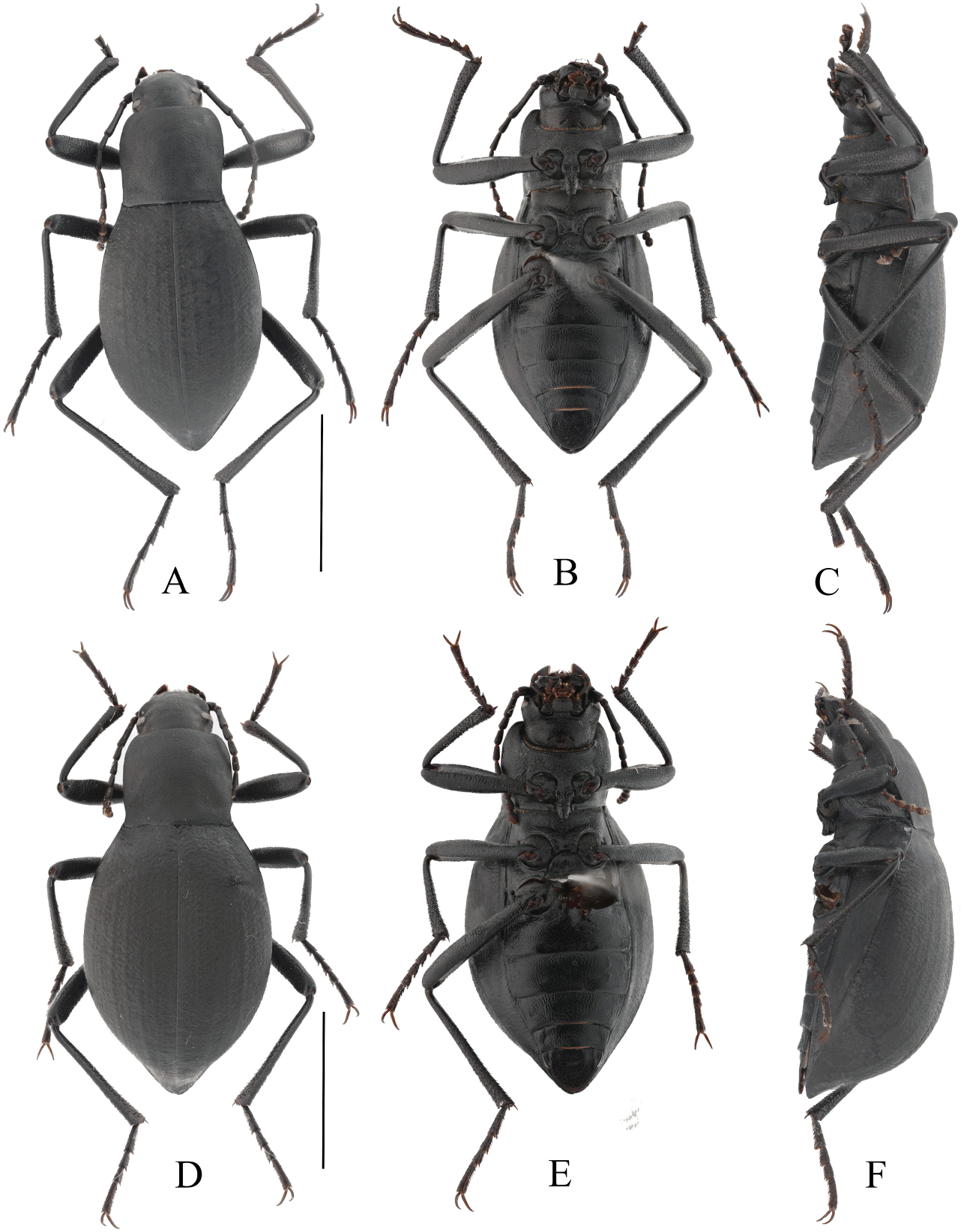

FIGURE 3. Habitus of *Blaps (Blaps) miranda* Li, **sp. nov. A–C.** Male, holotype: dorsal view (A). ventral view (B). lateral view (C). **D–F.** Female, paratype: dorsal view (D). ventral view (E). lateral view (F). Scale bars: 5.0 mm.

Prothorax (Fig. 2C). Base of pronotum as wide as the base of elytra. Pronotum with subequal length and width, widest at middle, 1.5 times as wide as head, lateral margins from widest portion toward anterior angles arcuated, then straightly converging towards base, where slightly divergent; lateral edges entirely margined, ratio of width at anterior margin to widest part and base 68: 85: 80. Disc convex, surface with dense puncturation. Prosternal process distinctly projecting beyond the margin of prosternum, flat on both sides; apex of prosternal process sharp, and projecting on middle.

Pterothorax. Elytra ovoid, 1.5 times as long as wide, widest at the middle, 2.5 times as long and 1.5 times as wide as pronotum, 2.3 times as wide as head. Lateral elytral border not entirely visible dorsally. Scutellum small. Disc convex, dull, elytral surface rough, with sparse granules. Apex of elytra steeply sloping. Without elytral mucro.

Legs (Fig. 2E–K). Legs long, profemora slender, inner side of pro- and mesotibiae slightly curved, expanded apically. Ratio of length of pro-, meso- and metatibiae 11: 12: 15; ratio of length (width) of metatarsomeres I–IV 16.3 (4.8): 10.0 (4.5): 9.9 (4.3): 19.4 (4.8).

Abdomen shiny, without hair tuft/short setae between 1st and 2nd abdominal ventrites, 1st–3rd with transverse/ longitudinal wrinkles, abdominal ventrites 4 and 5 with sparse punctures. Aedeagus (Fig. 2L–N). Length 2.6 mm and width 0.6 mm. Parameres length 0.75 mm and width 0.5 mm, bottleneck-shaped, apex acuminate; parameres wide and convex at base, lateral margin arcuately converging from base to middle and flat on both sides, then straightly converging from middle to apex in dorsal view; parameres slightly curved to ventral side apically in lateral view.

Female (Fig. 3D–F). Body length 17.5–18mm, width 7.5–8 mm. Body wider than male. Head as wide as outerocular distance, pronotum 1.1 times as wide as long, elytra 1.4 times as long as wide. Antennae shorter than in male, antennomere XI reaching base of pronotum when directed backward. Pronotum and elytra more convex. Before the base of lateral margin of pronotum concave. Inner side of pro- and mesotibiae slightly curved, expanded apically.

Etymology. Miranda is a feminine noun, name of Latin origin, meaning "worthy of admiration".

Distribution. China: Xizang.

Diagnosis. The new species is morphologically very similar to *B.* (*A.*) *gentilis gentilis* Fairmaire, 1887, but can be distinguished from the latter by the following male characters: (1) disc of elytral convex, with sparse and fine granules (disc of elytral flat, with coarse granules in *B.* (*A.*) *gentilis gentilis*); (2) parameres bottleneck-shaped, slightly curved to ventral side apically in lateral view (parameres conical-shaped, curved to dorsal side apically in lateral view in *B.* (*A.*) *gentilis gentilis*) (Skopin & Kaszab 1978).

Blaps (*Ablapsis*) *gracilis* Li, sp. nov.

urn:lsid:zoobank.org:act:96390153-FFAD-42A4-8EDD-EC605FF8795B

Type materials. HOLOTYPE: CHINA: ♂ (MHBU): 'Zito Township, Lhorong County, Xizang/ 30.5421°N, 95.7796°E/ Alt 4206m/ 30.VII.2019/ Xing-long Bai leg.'. **PARATYPES: CHINA:** 3 ♀♀ [in ethanol] (MHBU), same data as holotype.

Description. *Male* (Figs 4, 5A–C). Body slender, length 17–17.5 mm, width 5.5–6 mm; black, shinny.

Head (Fig. 4A, B). Anterior margin of epistome concave. Head slightly convex, with dense and coarse puncturation. Mentum transversely oval. Antennae long, antennomeres VIII reaching base of pronotum when directed backward, antennomeres III–VII cylindrical, VIII–X long spherical, XI spindle (Fig. 4D). Ratio of length (width) of antennomeres II–XI 6.0 (6.3): 29.3 (6.9): 13.4 (7.6): 12.8 (6.7): 14.4 (6.8): 15.8 (6.4): 10.0 (7.4): 10.3 (6.8): 10.6 (7.2): 14.1 (6.9).

Prothorax (Fig. 4C). Pronotum nearly square shaped, 1.1 times as wide as long, widest before the middle 1.6 times as wide as head, lateral margins from widest portion toward anterior angles arcuated, then straightly converging towards posterior margin; ratio of width at anterior margin to the middle part and base 28: 45: 40. Disc smooth, surface with sparse, fine puncturation. Prosternal process nearly triangular; apex of prosternal process straight.

Pterothorax. Elytra elongate, ovoid, widest at the middle, weakly long arcuated, 1.9 times as long as wide, 2.8 times as long and 1.3 times as wide as pronotum, 2.1 times as wide as head. Lateral elytral border not entirely visible dorsally. Scutellum small. Disc flat, shiny, elytral with rasp-shaped punctation and microgranules. Apex of elytra obtuse. Elytra without mucro.

Legs (Fig. 4E–K). Legs long. Inner side of pro-, meso- and metatibiae slightly curved, expanded apically. Ratio of length of pro-, meso- and metatibiae 45: 42: 57; ratio of length (width) of metatarsomeres I–IV 16.9 (4.4): 10.0 (4.1): 8.6 (3.6): 15.5 (4.0).

Abdomen shiny, without hair tuft/short setae between 1st and 2nd abdominal ventrites, abdominal ventrites 4 and 5 with sparse punctures and long recumbent setae. Aedeagus (Fig. 4L–N). Length 4.4 mm and width 1 mm. Parameres length 1 mm and width 0.5 mm, parameres wide and convex at base, gourd-shaped, apex obtuse; lateral margin weakly converging from base to apex and weakly concave at 1/3 of base in dorsal view; parameres flat from apex to middle, then slightly convex to base in lateral view.

Female (Fig. 5D–F)**.** Body length 19–19.5mm, width 7–7.5 mm. Body wider and more robust than male. Head as wide as outerocular distance, pronotum 1.1 times as wide as long, elytra 1.6 times as long as wide. Antennae shorter than in male, antennomere IX reaching base of pronotum when directed backward. Elytra with dense puncturation and microgranules.

Etymology. This species is named from the Latin adjective "gracilis", in reference to body slender.

Distribution. China: Xizang.

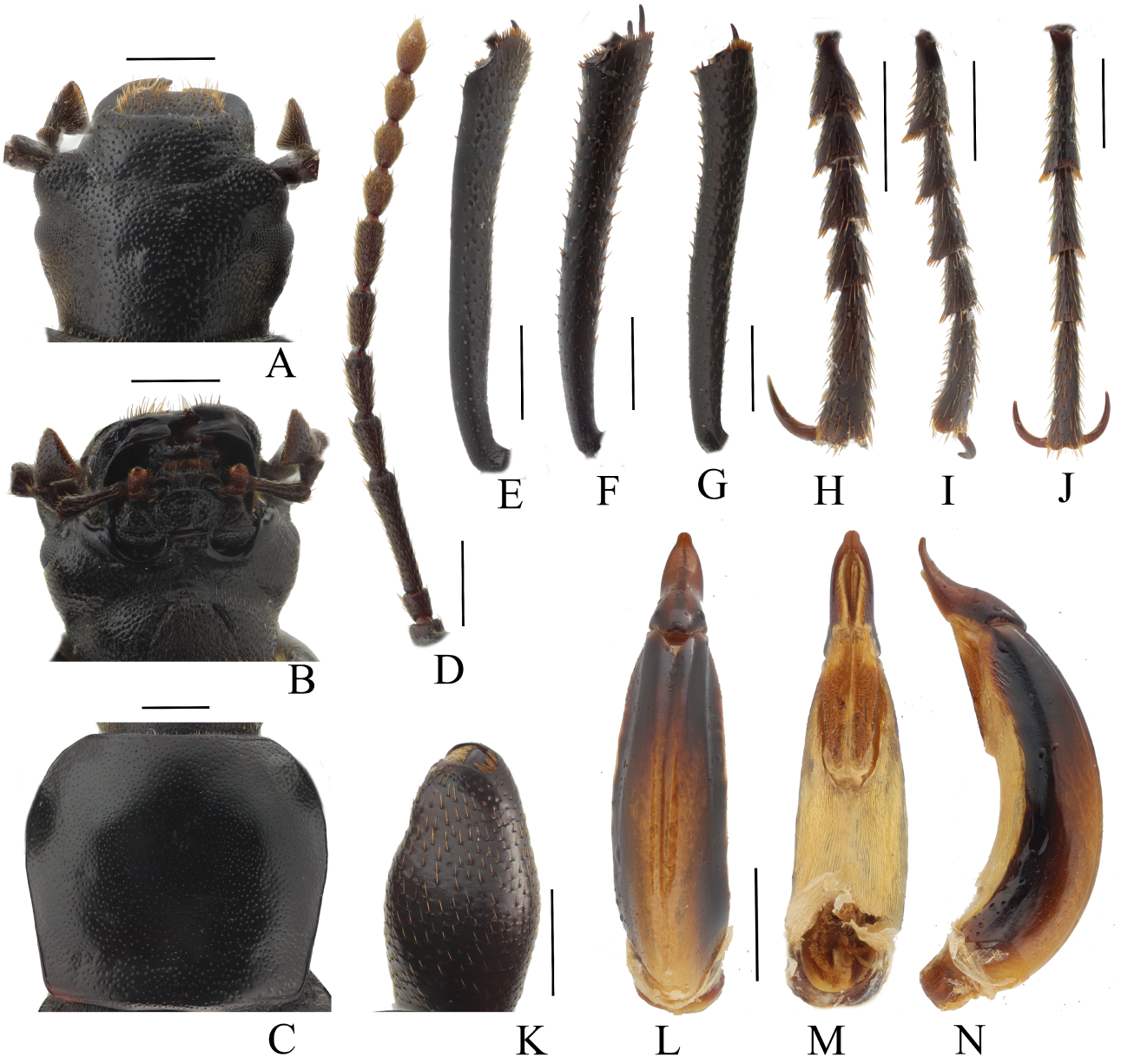

FIGURE 4. *Blaps* (*Ablapsis*) *gracilis* Li, **sp. nov. A.** Head, dorsal view. **B.** Head, ventral view. **C.** Pronotum. **D.** Antenna. **E.** Protibia. **F.** Mesotibia. **G.** Metatibia. **H.** Protarsus. **I.** Mesotarsus. **J.** Metatarsus. **K.** Profemur, apical part. **L–N**. Aedeagus: dorsal (L), ventral (M), lateral (N). Scale bars: 1.0 mm.

Diagnosis. The new species is morphologically similar to *B.* (*A.*) *berezowskii* Medvedev, 1998, but can be distinguished from the latter by the following male characters: (1) elytral with rasp-shaped punctation and microgranules (elytral with inconspicuous coarse granules in *B.* (*A.*) *berezowskii*); (2) apex of elytra obtuse (apex of elytra acute in *B.* (*A.*) *berezowskii*); (3) parameres without deep depression in dorsal view (parameres with one deep depression in dorsal view in *B.* (*A.*) *berezowskii*).

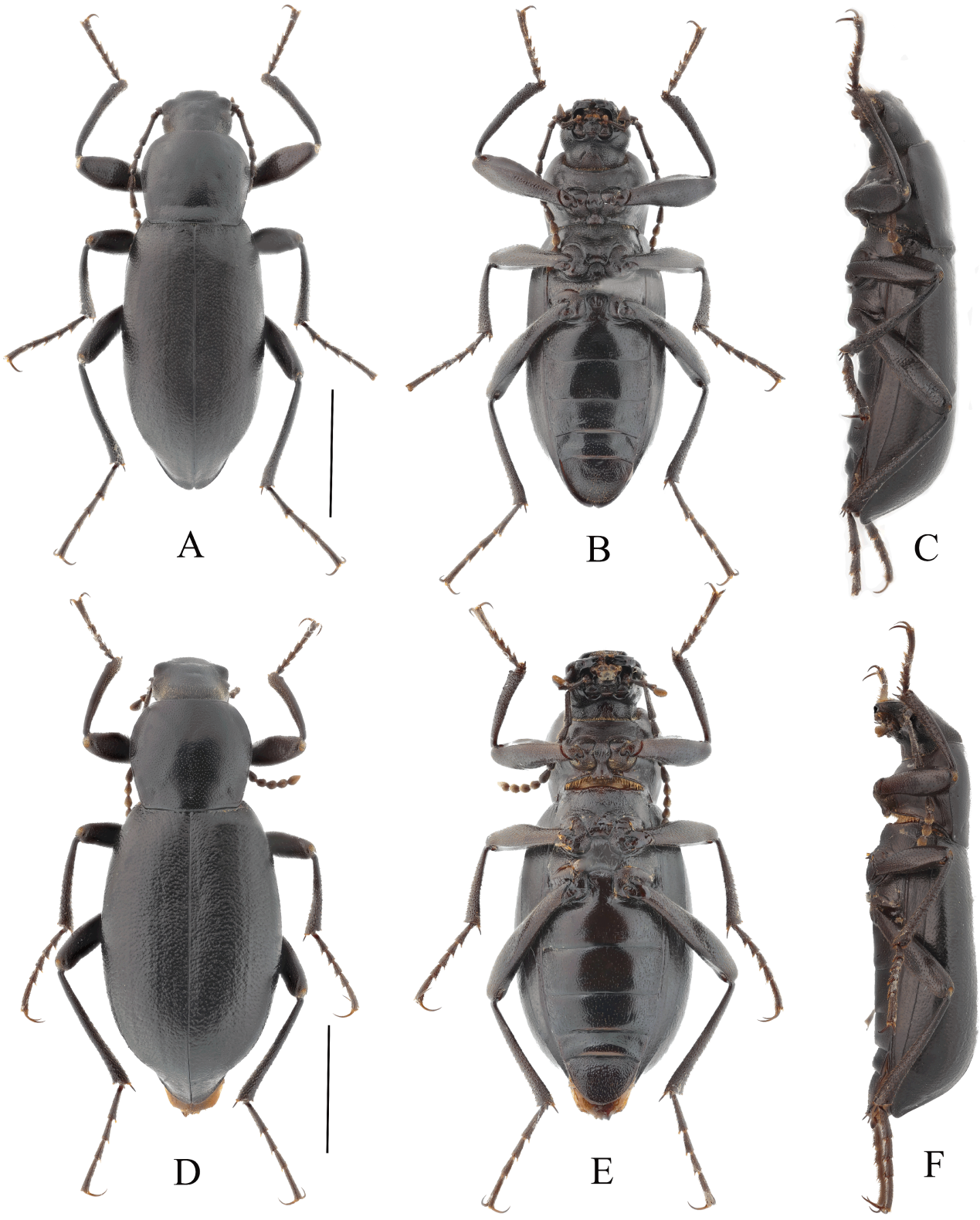

FIGURE 5. Habitus of *Blaps* (*Ablapsis*) *gracilis* Li, **sp. nov. A–C.** Male, holotype: dorsal view (A). ventral view (B). lateral view (C). **D–F.** female, paratype: dorsal view (D). ventral view (E). lateral view (F). Scale bars: 5.0 mm.

***Blaps* (*Ablapsis*) *asperula* Li, sp. nov.**
urn:lsid:zoobank.org:act:629A21FD-ADAF-4151-8042-4055A06A159D

Type materials. HOLOTYPE: CHINA: ♂ (MHBU): 'Lugula Shan, Xizang/ 8.VIII.2014/ Guo-dong Ren leg.'. **PARATYPES: CHINA:** 1 ♀ [in ethanol] (MHBU), same data as holotype; 2 ♂♂ [in ethanol] (MHBU): 'Nagarzê County, Xizang/ 6.VIII.2014/ Guo-dong Ren leg.'.; 1 ♂ [in ethanol] (MHBU): 'Chigu Township, Comai County, Xizang/ 8.VIII.2014/ Guo-dong Ren leg.'; 1 ♂ [in ethanol] (MHBU): 'Pagri Township, Yadong County, Xizang/ 27.7963°N, 89.1467°E/ Alt 4359m/ 11.VI.2018/ Xing-long Bai leg.'.

Description. *Male* (Figs 6, 7A–C). Body length 18.5–19.5 mm, width 7–8 mm; dull black, rough, opaque.

Head (Fig. 6A, B). Anterior margin of epistome straight. Head slightly convex, with dense and coarse puncturation. Mentum transversely oval. Antennae reaching base of pronotum when directed backwards, antennomeres III–VI cylindrical, VII subconical, VIII–X spherical, XI spindle (Fig. 6D). Ratio of length (width) of antennomeres II–XI 5.8 (7.6): 28.9 (8.7): 10.7 (8.1): 11.9 (7.9): 10.0 (7.5): 13.1 (10.0): 7.7 (9.3): 8.5 (10.6): 8.8 (10.3): 12.8 (10.4).

Prothorax (Fig. 6C). Pronotum slightly transverse, 1.3 times as wide as long, widest before the middle 1.3 times as wide as head, lateral margins from widest portion toward anterior angles arcuated, then straightly converging towards posterior margin; ratio of width at anterior margin to widest part and base 5.8: 10: 7.9. Disc weakly convex, surface with coarse puncturation. Prosternal process nearly triangular; apex of prosternal process straight.

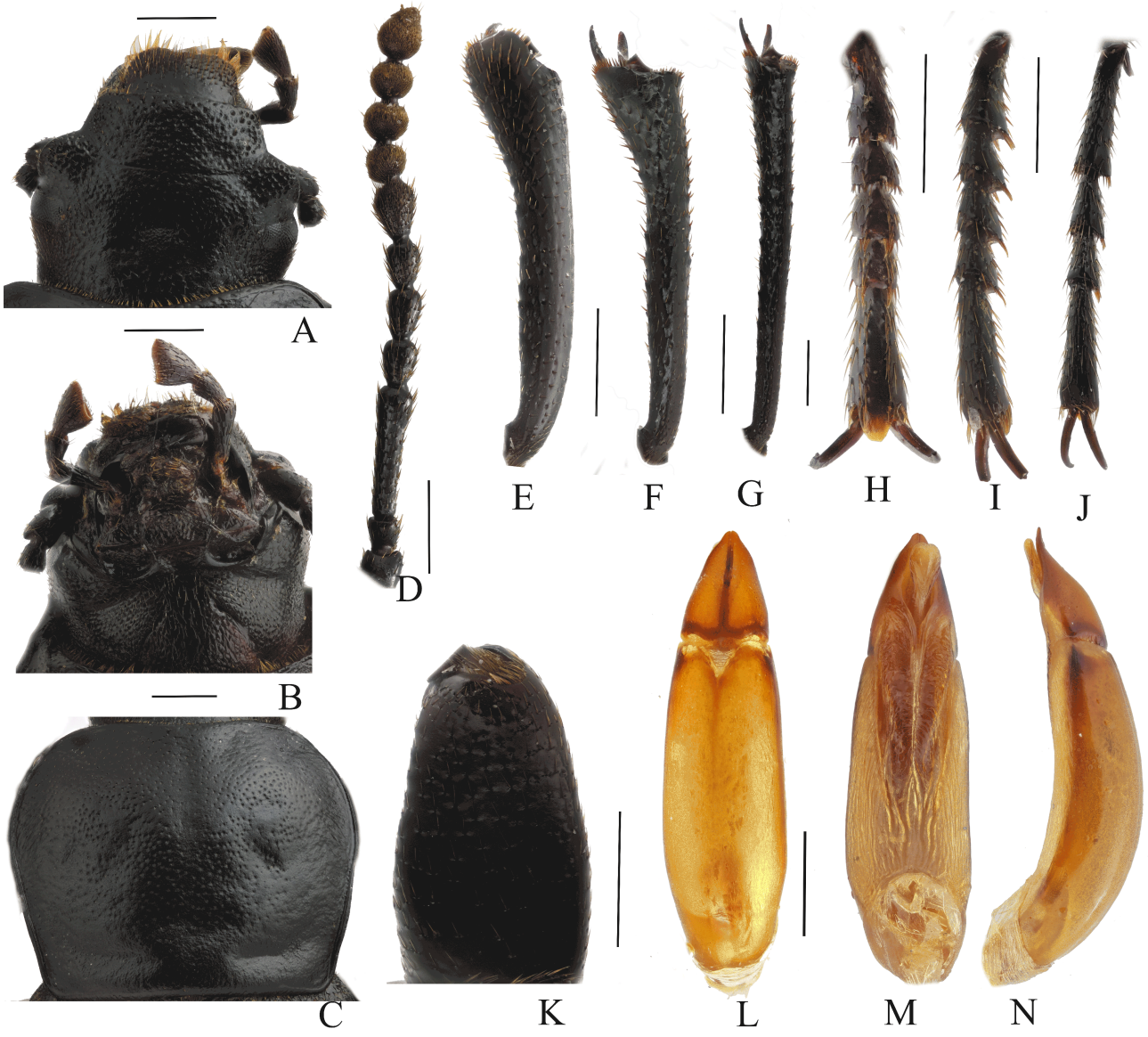

FIGURE 6. *Blaps* (*Ablapsis*) *asperula* Li, **sp. nov. A.** Head, dorsal view. **B.** Head, ventral view. **C.** Pronotum. **D.** Antenna. **E.** Protibia. **F.** Mesotibia. **G.** Metatibia. **H.** Protarsus. **I.** Mesotarsus. **J.** Metatarsus. **K.** Profemur, apical part. **L–N**. Aedeagus: dorsal (L), ventral (M), lateral (N). Scale bars: 1.0 mm.

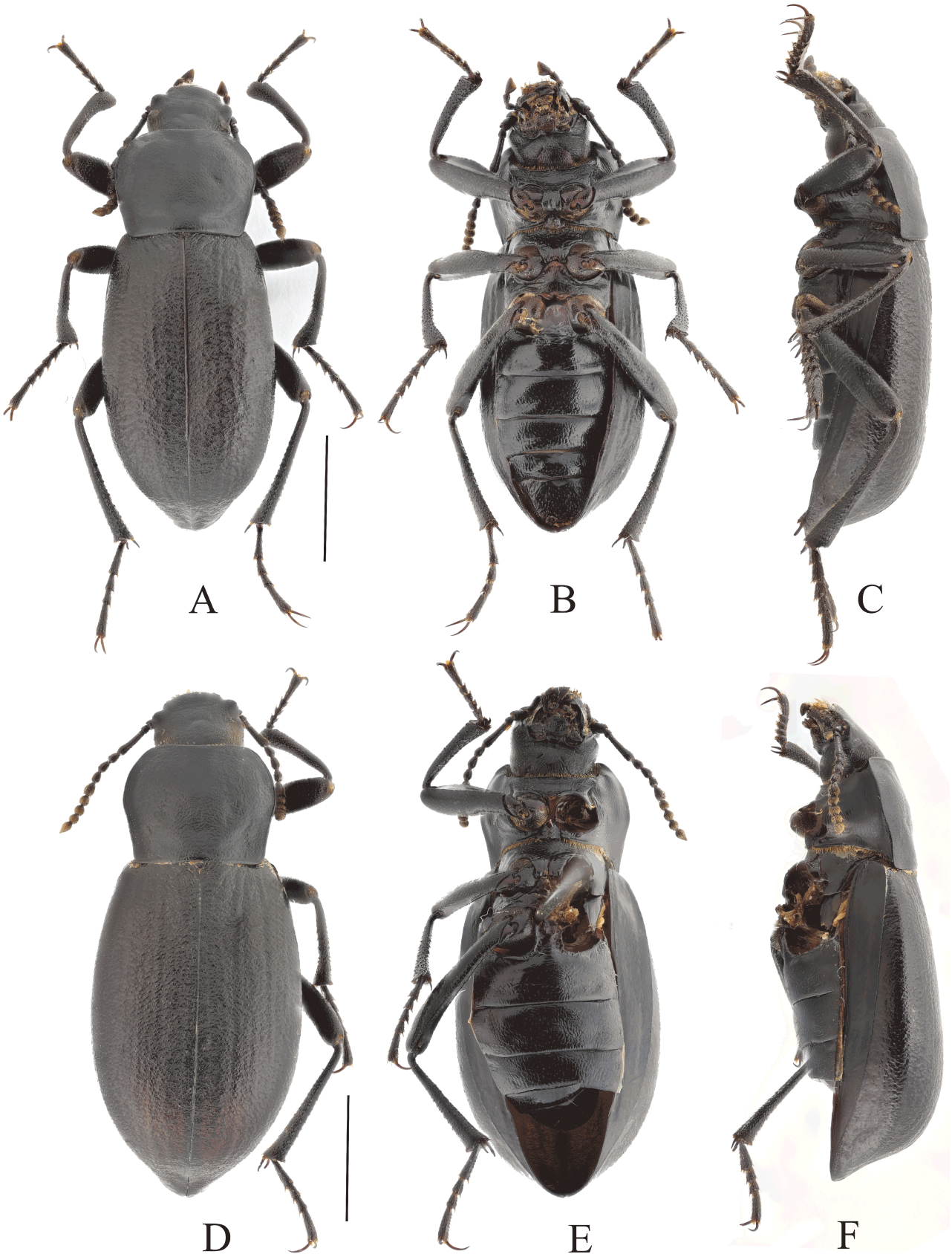

FIGURE 7. Habitus of *Blaps (Ablapsis) asperula* Li, **sp. nov. A–C.** Male, holotype: dorsal view (A). ventral view (B). lateral view (C). **D–F.** Female, paratype: dorsal view (D). ventral view (E). lateral view (F). Scale bars: 5.0 mm.

Pterothorax. Elytra elongate, ovoid, widest at the middle, weakly arcuated, 1.7 times as long as wide, 2.9 times as long and 1.2 times as wide as pronotum, 2.1 times as wide as head. Full length of the rim is invisible from the dorsal view. Scutellum small. Disc coarse, elytral surface with obvious irregular granular wrinkles. Apex of elytra obliquely sloping. Elytra without mucro.

Legs (Fig. 6E–K). Inner side of pro- and mesotibiae curved, expanded apically. Ratio of length of pro-, meso- and metatibiae 46: 50: 65; ratio of length (width) of metatarsomeres I–IV 22.9 (6.2): 10.8 (5.9): 10.0 (5.9): 22.7 (7.2).

Abdomen shiny, without hair tuft/short setae between 1st and 2nd abdominal ventrites, abdominal ventrites 4 and 5 with sparse punctures

Aedeagus (Fig. 6L–N). Length 4.5 mm and width 1 mm. Parameres length 1.2 mm and width 0.8 mm, parameres widest at the base, conical-shaped, apex obtuse; lateral margin weakly converging from base to apex in dorsal view; parameres flat from apex to 1/3, then weakly convex to base in lateral view; slightly curved to dorsal side apically in lateral view.

Female (Fig. 7D–F)**.** Body length 19.5–20.5mm, width 8–9 mm. Body wider than male. Head as wide as outerocular distance, pronotum 1.3 times as wide as long, elytra 1.6 times as long as wide. Antennae shorter than in male, not reaching base of pronotum when directed backwards. Elytra with dense granules, without wrinkles.

Etymology. This species is named from the Latin adjective “asperula” (rough), in reference to its pterothorax with coarse sculpture.

Distribution. China: Xizang.

Diagnosis. The new species is morphologically very similar to *B.* (*A.*) *brevis* Ren et Wang, 2001, but can be distinguished from the latter by the following male characters: (1) pronotum slightly transverse, widest before the middle (pronotum transverse, widest at the middle in *B.* (*A.*) *brevis*); (2) elytra surface coarse, with obvious irregular granules and wrinkles (elytra surface with dense granules in*B.* (*A.*) *brevis*); (3) parameres conical-shaped, apex obtuse (parameres needle-shaped, apex sharp in *B.* (*A.*) *brevis*).

Blaps (*Ablapsis*) *tuberculata* Li, sp. nov.

urn:lsid:zoobank.org:act:98509EB1-5EB6-4994-B9D9-0552D252774A

Type materials. HOLOTYPE: CHINA: ♂ **(MHBU**): ‘Bayi Zhen, Nyingchi County, Xizang/ 29.6653°N, 94.3428°E/ Alt 2995m/ 10.VIII.2018/ Xing-long Bai leg.’. **PARATYPES: CHINA:** 1 ♂, 1 ♀ [in ethanol] (MHBU), same data as holotype; 2 ♂♂, 4 ♀♀ [in ethanol] (MHBU): ‘Mainling County, Xizang/ 29.1864°N, 94.1961°E/ Alt 2930m/ 27.VII.2019/ Xiu-min Li leg.’; 2 ♀♀ [in ethanol] (MHBU): ‘Bomê County, Xizang/ 29.8203°N, 94.7869°E/ Alt 2775m/ 24.VII.2022/ Guo-dong Ren leg.’.

Description. *Male* (Figs 8, 9A–C). Body length 23–23.5mm, width 8–8.5mm; black, dull.

Head (Fig.8A, 8B). Anterior margin of epistome straight. Head convex, with sparse puncturation. Mentum transversely oval. Antennae long, antennomeres IX reaching base of pronotum when directed backwards, antennomeres I–VII cylindrical, VIII–X long spherical, XI spindle (Fig. 8D). Ratio of length (width) of antennomeres II–XI 10.0 (11.4): 52.2 (12.8): 19.2 (11.0): 21.6 (10.8): 21.5 (11.0): 23.5 (11.4): 14.9 (12.8): 15.2 (13.9): 15.0 (14.1): 18.8 (12.8).

Prothorax (Fig. 8C). Pronotum square shaped, 1.1 times as wide as long, widest before the middle, 1.7 times as wide as head, lateral margins from widest portion toward anterior angles arcuated, then straightly converging towards posterior margin; Ratio of width at anterior margin to -widest part and base 6.7: 10: 8.2. Disc smooth, surface with dense and fine puncturation. Prosternal process nearly rhombic; apex of prosternal process sharp.

Pterothorax. Elytra elongate, ovoid, widest at the middle, weakly arcuated, 1.7 times as long as wide, 2.6 times as long and 1.3 times as wide as pronotum, 2.1 times as wide as head. Lateral elytral border not entirely visible dorsally. Scutellum small. Disc convex, elytral surface rough, with dense fine granules. Apex of elytra steeply sloping. Elytra without mucro. Pseudopleuron with uniformly distributed small particles.

Legs (Fig. 8E–K). Profemora slender, inner side of protibiae slightly curved, expanded apically. Ratio of length of pro-, meso- and metatibiae 12: 13: 17, ratio of length (width) of metatarsomeres I–IV 28.1 (7.2): 11.8 (6.6): 10.0 (6.2): 20.9 (6.8).

Abdomen shiny, without hair tuft/short setae between 1st and 2nd abdominal ventrites, 1st–3rd with transverse/ longitudinal wrinkles and small particles on both sides, abdominal ventrites 4 and 5 with punctures.

FIGURE 8. *Blaps* (*Ablapsis*) *tuberculata* Li, **sp. nov. A.** Head, dorsal view. **B.** Head, ventral view. **C.** Pronotum. **D.** Antenna. **E.** Protibia. **F.** Mesotibia. **G.** Metatibia. **H.** Protarsus. **I.** Mesotarsus. **J.** Metatarsus. **K.** Profemur, apical part. **L–N**. Aedeagus: dorsal (L), ventral (M), lateral (N). Scale bars: 1.0 mm.

Aedeagus (Fig. 8L–N). Length 6.2 mm and width 1 mm. Parameres length 1.8 mm and width 0.7 mm, parameres widest at base, nail-shaped, apex obtuse; lateral margin arcuately converging from base to basal 1/5, then weakly converging to apex, the 3/5 of the middle weakly concave in dorsal view; slightly curved to dorsal side apically in lateral view; parameres slightly curved, narrowed almost in a straight line up to apex in lateral view.

Female (Fig. 9D–F)**.** Body length 22–23 mm, width 9–9.5 mm. Body wider than male. Head as wide as outerocular distance, pronotum 1.2 times as wide as long, elytra 1.6 times as long as wide. Antennae shorter than in male, not reaching base of pronotum when directed backwards, antennomeres VIII–X spherical. Apex of elytra with 2–3 longitudinal ridges.

Etymology. This species is named from the Latin noun "*tubercŭlum*", in reference to its elytra with dense and fine granules.

Distribution. China: Xizang.

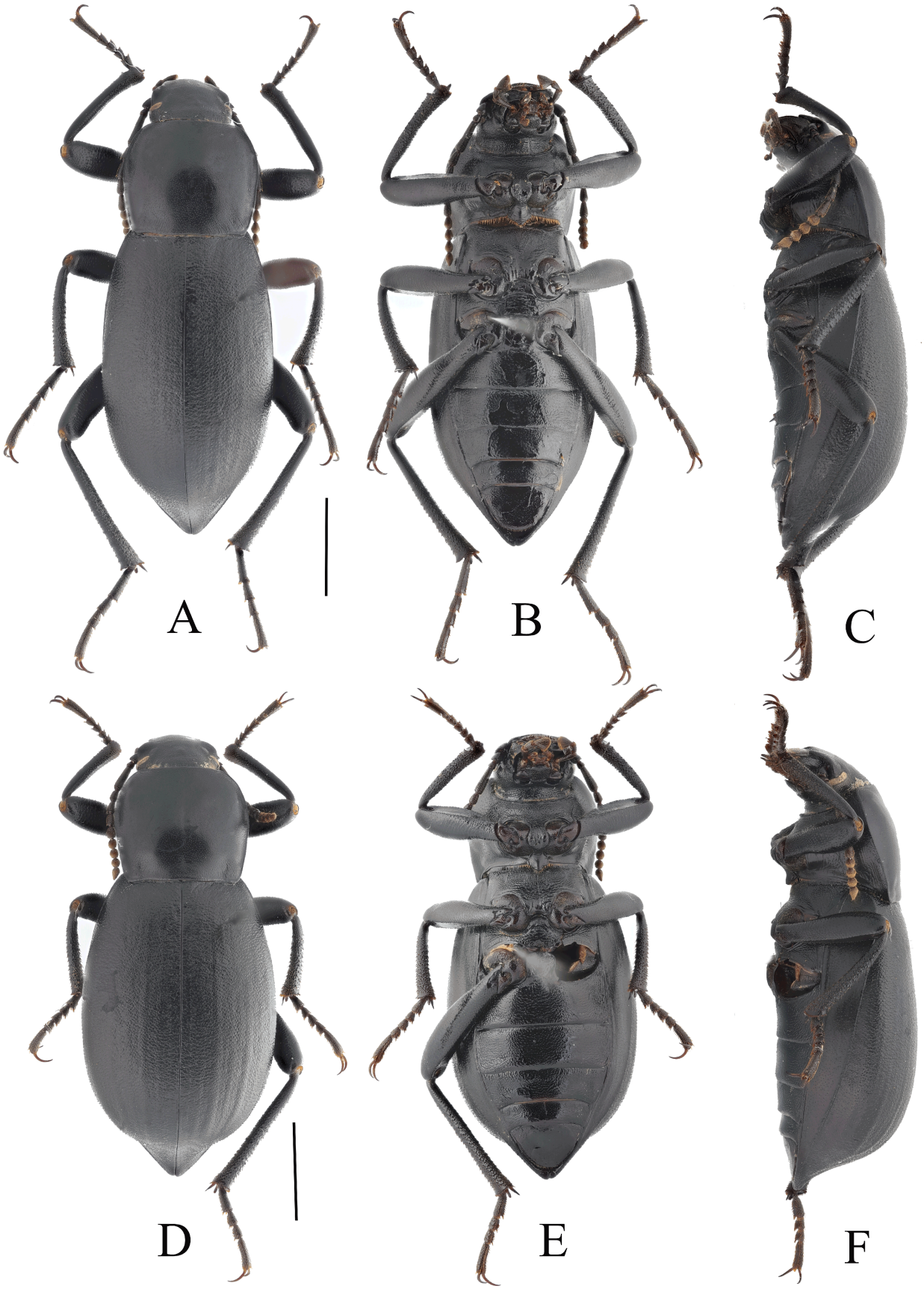

FIGURE 9. Habitus of *Blaps (Ablapsis) tuberculata* Li, **sp. nov. A–C.** Male, holotype: dorsal view (A). ventral view (B). lateral view (C). **D–F.** Female, paratype: dorsal view (D). ventral view (E). lateral view (F). Scale bars: 5.0 mm.

Diagnosis. The new species is morphologically very similar to *B.*(*A.*) *holcus* Ren, 2016, but can be distinguished from the latter by the following male characters: (1) antennae long, antennomeres longer than base of pronotum when directed backwards, antennomeres VIII–X long spherical (antennae shorter, not reaching base of pronotum when directed backwards, antennomeres VIII–X spherical in *B.*(*A.*) *holcus*); (2) pronotum widest before the middle (widest at the middle in *B.*(*A.*) *holcus*); (3) inner side of protibiae slightly curved (inner side of protibiae straight in *B.*(*A.*) *holcus*); (4) parameres nail-shaped, the 3/5 of the middle weakly concave in dorsal view (parameres needle-shaped, weakly converging form base to apex in dorsal view in *B.*(*A.*) *holcus*).

Discussion

Blaps is the most species-rich genus within the subtribe Blaptina, with 205 described species, primarily distributed in the Palaearctic region (Nabozhenko & Chigray 2020). These species inhabit a range of environments, including desert, semi-desert, meadow and shrublands, cave and other habitats, exhibiting high species diversity and extensive distribution. Research suggests that *Blaps* is likely polyphyletic based on molecular data (Soldati *et al*. 2017; Condamine *et al*. 2013; Li *et al*. 2023; Zhang & Li 2025). In this study, we observed considerable diversity in the aedeagal morphology of *Blaps* across different habitats. The subgenera *Ablapsis* and *Nalepa* represent monophyletic group. However, the species of *Ablapsis* share a common characteristic: the smaller parameres relative to the basal piece of the aedeagus, which curved to dorsally at the apex in lateral view (Chigray & Kirejtshuk 2023). In contrast, the parameres of the subgenus *Nalepa* are either straight or slightly curved ventrally at the apex in lateral view, predominantly taking on conical or bottleneck shaped (Li *et al.* 2022). Notably, the species of the subgenus *Blaps* from China form five paraphyletic clades. We examined the shape of parameres within each clade and found common traits: species of Clade C6 possess conical-shaped parameres, which inhabit desert areas in northwest China. Species of the subgenus *Blaps* on Clade C7 are also distributed in the desert area of northwest China. The remaining clades, which are also paraphyletic, primarily inhabit high-altitude regions of the Tibetan Plateau. The subgenus *Blaps* consists of 182 species and subspecies, representing the largest distribution area. Resolving the taxonomic status of subgenera within the genus *Blaps* remains a challenge. Future research should focus on accumulating extensive molecular datasets and integrating morphological characteristics of Blaptini to clarify the taxonomic status of the subgenus *Blaps* and the genus *Blaps*.

Acknowledgments

This research was funded by the National Natural Science Foundation of China (32170477), the Natural Science Foundation of Hebei (C2024201003). We are grateful to the editor and anonymous reviewers for their constructive comments on the manuscript.

References

Condamine, F.L., Soldati, L., Clamens, A.L., Rasplus, J.Y. & Kergoat, G.J. (2013) Diversification patterns and processes of wingless endemic insects in the Mediterranean Basin: historical biogeography of the genus *Blaps* (Coleoptera: Tenebrionidae). *Journal of Biogeography*, 40 (10), 1899–1913. https://doi.org/10.1111/jbi.12144

Chigray, I. & Kirejtshuk, A. (2023) The supraspecific structure of the subtribe Blaptina Leach, 1815 (Coleoptera, Tenebrionidae: Blaptinae). *Acta Zoologica Academiae Scientiarum Hungaricae*, 69 (3), 213–245. https://doi.org/10.17109/AZH.69.3.213.2023

Egorov, L.V. (2009) *Tenebrionids of the tribe Platyscelidini (Coleoptera, Tenebrionidae) of the world fauna: morphology, zoogeography, systematics*. *Iss. 61 (1)*. Russian Entomological Society Publ., Saint Petersburg, 332 pp. [in Russian]

Folmer, O., Black, M., Hoeh, W., Lutz, R. & Vrijenhoek, R. (1994) DNA primers for amplification of mitochondrial cytochrome c oxidase subunit I from diverse metazoan invertebrates. *Molecular marine biology and Biotechnology*, 3 (5), 294–299.

Kamiński, M.J., Lumen, R., Kanda, K., Iwan, D., Johnston, M.A., Kergoat, G.J., Bouchard, P., Bai, X.L., Li, X.M., Ren, G.D. & Smith, A.D. (2021) Reevaluation of Blapimorpha and Opatrinae: addressing a major phylogeny-classification gap in darkling beetles (Coleoptera: Tenebrionidae: Blaptinae). *Systematic Entomology*, 46 (1), 140–156. https://doi.org/10.1111/syen.12453

Li, X.-M., Tian, J., Fan, J.-J. & Ren, G.-D. (2022) Systematic review of the genus *Nalepa* Reitter, 1887 (Coleoptera, Tenebrionidae, Blaptinae, Blaptini) from the Tibetan Plateau, with description of six new species and two larvae. *Insects*, 13, 598. https://doi.org/10.3390/insects13070598

Li, X.-M., Ji, B., Tian, J. & Ren, G.-D. (2023) The adult and larva of a new species of the genus *Dila* (Coleoptera, Blaptinae, Blaptini) from Himalayas, with molecular phylogenetic inferences of related genera of the Blaptini. *Insects*, 14, 284. https://doi.org/10.3390/insects14030284

Minh, B.Q., Nguyen, M.A.T. & Von Haeseler, A. (2013) Ultrafast approximation for phylogenetic bootstrap. *Molecular Biology and Evolution*, 30 (5), 1188–1195. https://doi.org/10.1093/molbev/mst024

Medvedev, G.S. (2001) *Evolution and system of darkling beetles of the tribe Blaptini (Coleoptera, Tenebrionidae)*. *Iss. 53*. Russian Entomological Society Publ., Saint Petersburg, 332 pp. [in Russian]

Nabozhenko, M. & Chigray, I. (2020) Tribe Blaptini Leach, 1815. *In*: Iwan, D. & Löbl, I. (Eds.), *Catalogue of Palaearctic Coleoptera*. *Vol 5*. *Tenebrionoidea. 2nd Edition.* KWoninklijke Brill NV, Leiden/Boston, pp. 268–296. https://doi.org/10.1163/9789004434998_004

Nguyen, L.T., Schmidt, H.A., Von Haeseler, A. & Minh, B.Q. (2015) IQ-TREE: A fast and effective stochastic algorithm for estimating maximum-likelihood phylogenies. *Molecular Biology and Evolution*, 32 (1), 268–274. https://doi.org/10.1093/molbev/msu300

Reitter, E. (1887) Insecta in itinere Cl. N. Przewalskii in Asia Centrali novissime lecta. ix. Tenebrionidae. *Horae Societatis Entomologicae Rossicae*, 21, 355–389.

Reitter, E. (1893) Ueber die Genus Charaktere der Gattungen *Blaps* Fr., Prosodes Eschsch. und Verwandte. *Deutsche Entomologische Zeitschrift*, 1893, 313–316. https://doi.org/10.1002/mmnd.48018930213

Ren, G., Ba, Y., Liu, H., Niu, Y., Zhu, X., Li, Z. & Shi, A. (2016) *Coleoptera: Tenebrionidae (I); Fauna Sinica: Insecta Vol. 63*. Science Press, Beijing, 532 pp.

Skopin, N.G. & Kaszab, Z. (1978) Über die Arten der Gattung *Blaps* F. (Coleoptera, Tenebrionidae), gesammelt von Herrn Dr. W. Wittmer im Jahre 1976 in Kaschmir. *Folia Entomologica Hungarica*, 31 (2), 207–212.

Soldati, L., Condamine, F.L., Clamens, A.L. & Kergoat, G.J. (2017) Documenting tenebrionid diversity: progress on *Blaps* Fabricius (Coleoptera, Tenebrionidae, Tenebrioninae, Blaptini) systematics, with the description of five new species. *European Journal of Taxonomy*, 282, 1–29. https://doi.org/10.5852/ejt.2017.282

Zhang, D., Gao, F., Jakovlić, I., Zou, H., Zhang, J., Li, W.X. & Wang, G.T. (2020) PhyloSuite: An integrated and scalable desktop platform for streamlined molecular sequence data management and evolutionary phylogenetics studies. *Molecular Ecology Resources*, 20 (1), 348–355. https://doi.org/10.1111/1755-0998.13096

Zhang, B.-Y. & Li, X.-M. (2025) Phylogeny-based reinterpretation of the genus *Blaps* Fabricius, 1775 (Coleoptera, Tenebrionidae, Blaptinae) from China, with description of two new species. *Zookeys*, 1244, 99–111. https://doi.org/10.3897/zookeys.1244.145585

Supplementary Materials. The following supporting information can be downloaded at the DOI landing page of this paper:

Table S1. List of specimens used in this study with the corresponding accession number.

西藏琵甲属*Blaps*四新种记述（鞘翅目：拟步甲科：琵甲亚科：琵甲族）

张宝月[1,2]，李欣雨[1,3]，李秀敏[1,4,*]
[1]河北大学生命科学学院，河北省动物系统学与应用重点实验室，保定，河北071002，中国
[2] BaoyueZhang0112@163.com; https://orcid.org/0009-0008-9251-479
[3] lixinyu01313@163.com; https://orcid.org/0009-0009-0400-0132
[4] lixiumin@hbu.edu.cn; https://orcid.org/0000-0003-0575-1869
[*]通讯作者

摘要：琵甲属*Blaps*是琵甲族中物种最丰富的一个属，包含214种。本文基于41个物种的线粒体基因片段（*COI*）初步构建了琵甲属系统发育树，其中内群38个物种种分别来自阿琵甲亚属、琵甲亚属和那琵甲亚属；还描述了西藏地区4新种，即奇异琵甲*Blaps* (*Blaps*) *miranda* **sp. nov.**、细粒琵甲*B.* (*Ablapsis*) *tuberculata* **sp. nov.**、粗糙琵甲*B.* (*A.*) *asperula* **sp. nov.** 和瘦琵甲*B.* (*A.*) *gracilis* **sp. nov.**；提供了阿琵甲亚属18个物种的种检索表。系统发育分析结果表明琵甲亚属可能是一个并系群，未来需深入研究以明确各亚属分类地位。

关键词：拟步甲，分子系统发育，新分类单元，分类